

REPORT

PALEOCLIMATE

Regional and global sea-surface temperatures during the last interglaciation

Jeremy S. Hoffman,^{1*}† Peter U. Clark,¹ Andrew C. Parnell,² Feng He^{1,3}

The last interglaciation (LIG, 129 to 116 thousand years ago) was the most recent time in Earth's history when global mean sea level was substantially higher than it is at present. However, reconstructions of LIG global temperature remain uncertain, with estimates ranging from no significant difference to nearly 2°C warmer than present-day temperatures. Here we use a network of sea-surface temperature (SST) records to reconstruct spatiotemporal variability in regional and global SSTs during the LIG. Our results indicate that peak LIG global mean annual SSTs were $0.5 \pm 0.3^\circ\text{C}$ warmer than the climatological mean from 1870 to 1889 and indistinguishable from the 1995 to 2014 mean. LIG warming in the extratropical latitudes occurred in response to boreal insolation and the bipolar seesaw, whereas tropical SSTs were slightly cooler than the 1870 to 1889 mean in response to reduced mean annual insolation.

The last interglaciation [LIG, 129 to 116 thousand years ago (ka)] was one of the warmest periods during the last 800,000 years (1), with an associated sea-level rise of 6 to 9 m above present levels (2). As such, the LIG provides an important target for validating global climate models used for climate-change projections (3, 4), as well as for understanding the sea-level response to a warm climate. However, the existing reconstructions of LIG global temperature needed to assess these issues suggest the possibility of no significant temperature change relative to the late Holocene to an increase of as much as 2°C (5–8). Moreover, these estimates either average temperature over part of or all of the LIG interval or assume that the warmest phases were globally synchronous, and these estimates do not account for systematic uncertainties in proxy calibrations and age estimates. As a result, these reconstructions are unable to constrain spatiotemporal variability in the response to the LIG climate forcing suggested by high-latitude compilations (9, 10).

Here we reconstruct regional and global sea-surface temperatures (SSTs) during the LIG that include a robust assessment of age model and proxy uncertainties. We compiled a near-global database of 104 published LIG SST records from 83 marine sediment core sites (Fig. 1A and tables S1 and S2). Of these records, 19 reflect summer

SSTs and 85 reflect mean annual SSTs (from 72 sites). The sample resolution ranges from centennial to <4000 years on their published age models, with a median resolution of 1100 years (fig. S1 and table S1).

We developed stratigraphically consistent chronologies for records from the South Atlantic, Indian, and Pacific basins by aligning representative high-southern latitude SST records from each basin (here referred to as reference cores) with the European Project for Ice Coring in Antarctica (EPICA) Dome C deuterium (δD) record on the Asian speleothem-based chronology (Speleo-Age model) (fig. S4) (11). We similarly aligned one North Atlantic SST record to the Greenland synthetic ice-core record that is also on the Speleo-Age model (fig. S4) (11). The highest correlations for lagged cross-correlations between model-based SSTs at the locations of our Southern Ocean reference cores and 2-m air temperatures over EPICA Dome C (EDC) are centered at zero lag (fig. S5), supporting this alignment strategy. We assigned the corresponding age model from each reference core to its benthic foraminiferal oxygen isotope ($\delta^{18}\text{O}$) record (fig. S6), which was then used for alignment with benthic $\delta^{18}\text{O}$ records from other cores in each basin (12) to account for potential interbasin variability in benthic $\delta^{18}\text{O}$ (13–15). A Bayesian age-depth modeling routine (Behron) (16) propagates the sources of age-model uncertainty for each record (12).

To compare proxy-based LIG SSTs with modern climatology, we referenced each core site in the database to the SST value in the nearest $1^\circ \times 1^\circ$ grid cell in the Version 1.1 of the Hadley Center Sea Ice and Sea Surface Temperature (HadISST1.1) 1870–1889 and 1995–2014 data sets (17) with the 1870–1889 period closely corresponding to pre-

industrial temperatures (18). We took the $5^\circ \times 5^\circ$ gridded, area-weighted mean of the SST records to develop regional and global LIG stacks of mean annual SSTs with 2σ uncertainties (Fig. 1). Assessment of the sensitivity of the global stack to the resolution, spatial averaging scheme, and number of records used in the stack suggests little to no influence (figs. S9 to S11). We also assessed proxy-dependent differences in the stack. On average, global stacks of geochemical proxies [ratio of magnesium to calcium (Mg/Ca) of planktonic foraminifera and the alkenone unsaturation index ($U^{K_{37}}$)] yield warmer SSTs than those of microfossil proxies (figs. S12 and S13). However, within uncertainties, there is good agreement between proxies within the same core for 12 existing comparisons (fig. S14). Similarly, proxy reconstructions within the same region are mostly in agreement and identify regionally coherent SST patterns (Fig. 2), suggesting that the difference in proxy-specific global stacks reflects spatial sampling bias. The one exception is the $U^{K_{37}}$ SST proxy that suggests a tendency for warmer tropical SSTs than either Mg/Ca or microfossil proxies (Fig. 2 and fig. S19). This may reflect a spring-summer dependence of $U^{K_{37}}$ and a bias toward higher unsaturation ratios (and thus warmer SSTs) in areas of dynamic oceanographic settings (19).

The global SST stack shows that the global ocean was already similar to the HadISST1.1 1870–1889 mean within uncertainties ($0.1^\circ \pm 0.3^\circ\text{C}$) at the onset of the LIG (129 ka) (Fig. 1E). There is a continuation of a warming trend from the penultimate deglaciation until 125 ka, when SSTs reached $0.5^\circ \pm 0.3^\circ\text{C}$ relative to the 1870–1889 mean and were indistinguishable ($0.1^\circ \pm 0.3^\circ\text{C}$) from the 1995–2014 mean (Fig. 1E). This warm LIG SST anomaly was followed by a cooling trend through the remainder of the LIG, reaching the HadISST1.1 1870–1889 mean by 120 ka as global climate approached the last glacial inception.

We estimate the thermal expansion of the ocean during the peak LIG warm interval from 10,000-year integrations with a coupled climate model (20). These model estimates yield an equilibrium sea-level change in the range of 0.42 to 0.64 m $^\circ\text{C}^{-1}$, suggesting a thermosteric contribution to the LIG sea-level high stand of 0.08 to 0.51 m. These estimates do not account for uncertainty in the different spatial distribution of the warming in models and the dependence of the expansion on local temperature and salinity.

Regional stacks and time-slice global maps reveal considerable regional differences in LIG SST anomaly timing, amplitude, and duration. The tropical (between 23.5°N and 23.5°S) SST stack has a structure similar to that of the global stack, but SSTs remained slightly below the HadISST1.1 1870–1889 mean throughout the LIG (Figs. 1G and 2), which is lower than in previous reconstructions (7, 8). If there is a warm bias in the $U^{K_{37}}$ proxy estimates (fig. S19), then tropical SSTs would be lower than suggested by our stack.

LIG SSTs in the extratropical regions of the southern and northern hemispheres (SH and NH, respectively) are significantly higher than

¹College of Earth, Ocean, and Atmospheric Sciences, Oregon State University, Corvallis, OR 97331, USA. ²School of Mathematics and Statistics, University College Dublin, Dublin 4, Ireland. ³Center for Climatic Research, Nelson Institute for Environmental Studies, University of Wisconsin–Madison, Madison, WI 53706, USA.

*Present address: Science Museum of Virginia, 2500 West Broad Street, Richmond, VA 23220-2057, USA. †Corresponding author. Email: jhoffman@smv.org

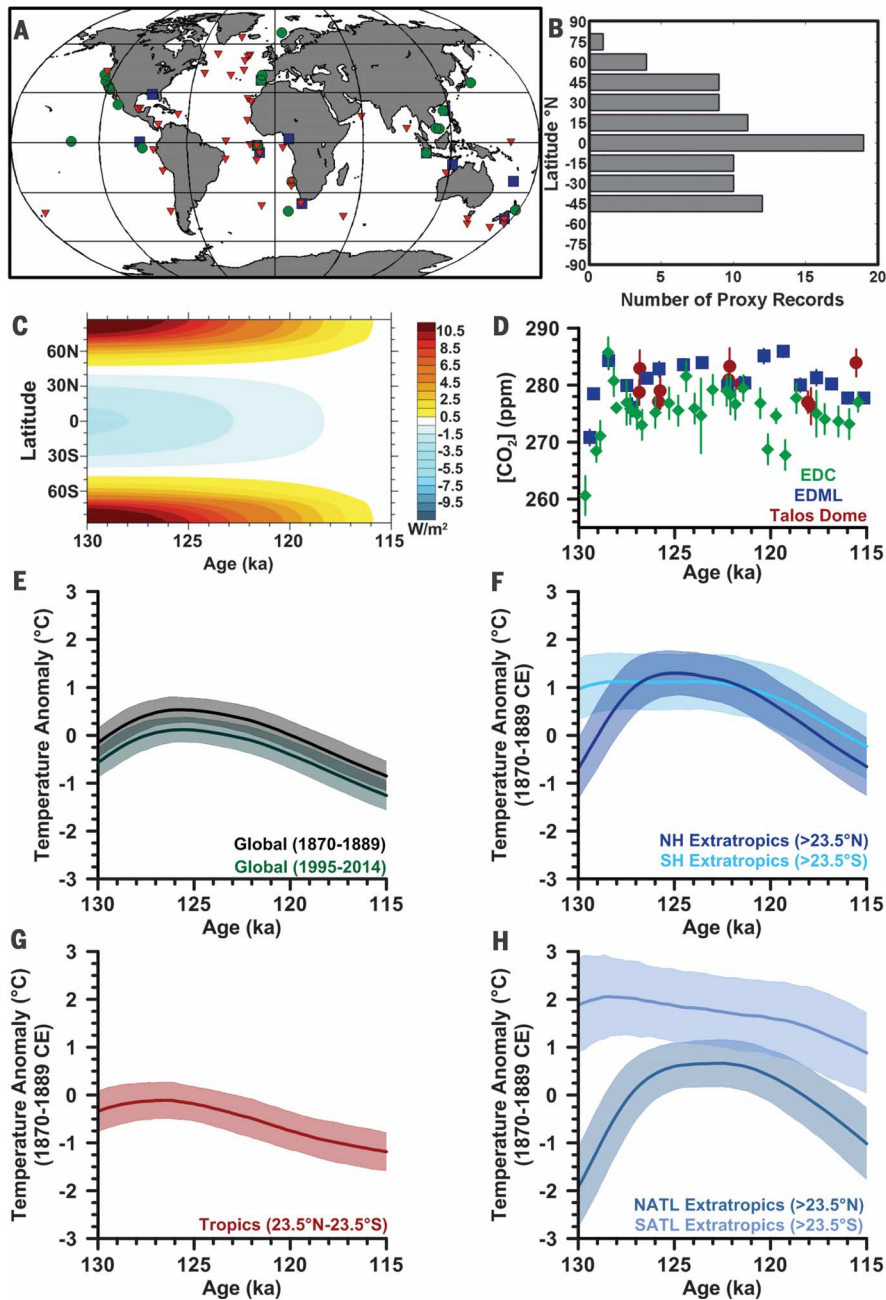


Fig. 1. Last interglacial proxy-based sea-surface temperature stacks, site locations, and climate context. (A) Site locations and types of proxy SST estimates included in this study. Symbols correspond to microfossil transfer functions (red triangles), Mg/Ca of planktonic foraminifera (green squares), and $U^{K_{37}}$ (blue circles). (B) Histogram relating the number of LIG proxy records to 15° latitude bins. (C) Contour plot of annual mean latitudinal insolation anomalies between 130 ka and 115 ka, relative to insolation at 115 ka. (D) Ice-core records of atmospheric CO₂ concentrations on Antarctic Ice Core Chronology 2012 (AICC2012) time scale, with one standard deviation on measurement. Symbols indicate records from EPICA Dome C (EDC) ice core (green diamonds) (30), Talos Dome ice core (red circles) (31), and EPICA Dronning Maud Land (EDML) ice core (blue squares) (31). (E) The global LIG 5° × 5° gridded, area-weighted mean annual SST stack relative to the HadISST1.1 1870–1889 mean (black line) and the HadISST1.1 1995–2014 mean (green line). (F) Extratropical (>23.5°N-S) mean annual SST stacks relative to the HadISST1.1 1870–1889 data. Dark blue, NH extratropics; light blue, SH extratropics. (G) The tropical (23.5°N-S) mean annual SST stack relative to the HadISST1.1 1870–1889 data. (H) The North Atlantic (NATL) and South Atlantic (SATL) extratropical mean annual SST stacks (sites >23.5°N-S within the Atlantic basin) relative to the HadISST1.1 1870–1889 data. The proxy-based SST stacks and their uncertainty are the 5° × 5° gridded, area-weighted mean and 2σ uncertainties of 1000 realizations used to construct the stacks.

the tropics (Figs. 1F, 2, and 3). However, SH and NH extratropical SSTs experienced distinctly different SST trajectories early in the LIG (Figs. 1F and 2A), in agreement with previous high-latitude reconstructions (10). In the SH extratropics, LIG SSTs that were $1.1^{\circ} \pm 0.6^{\circ}\text{C}$ greater than the 1870–1889 mean were already reached by 129 ka. SSTs remained near this level until 120 ka, when they then experienced a cooling trend that continued through the remainder of the LIG. NH extratropical SSTs show a similar LIG warming of $1.3^{\circ} \pm 0.5^{\circ}\text{C}$ relative to the 1870–1889 mean, but this warming was not reached until ~125 ka and was preceded by $1.3^{\circ} \pm 0.9^{\circ}\text{C}$ of warming since the start of the LIG. Subsequent cooling through the remainder of the LIG occurred at a similar rate in both high-latitude hemispheres.

The differences in these extratropical SST histories during the early LIG were even more pronounced in the Atlantic basin (Figs. 1H, 2, and 3). South Atlantic extratropical SSTs were $2.0^{\circ} \pm 0.9^{\circ}\text{C}$ higher than the 1870–1889 mean at 129 ka and cooled by $\sim 1.0^{\circ}\text{C}$ through the remainder of the LIG. In contrast, North Atlantic extratropical SSTs were $-1.2^{\circ} \pm 0.9^{\circ}\text{C}$ cooler than the 1870–1889 mean at 129 ka, increased during the early LIG to reach $0.6^{\circ} \pm 0.5^{\circ}\text{C}$ relative to the 1870–1889 mean at 125 ka, and were followed by a cooling trend that began at ~120 ka. Summer-specific proxies similarly suggest cooler summer SSTs in the North Atlantic extratropics early in the LIG followed by warmer SSTs at 125 ka (fig. S20).

Our results confirm that LIG global mean annual surface temperatures simulated with most global climate models forced with LIG boundary conditions (insolation and greenhouse gas concentrations) are too low (3, 4), with a multimodel estimate of $0.0^{\circ} \pm 0.5^{\circ}\text{C}$ at 125 ka (21) as compared to $0.5^{\circ} \pm 0.3^{\circ}\text{C}$ in our SST reconstruction. One recent simulation for 125 ka found global mean warming of 0.5°C with a spatial pattern similar to our reconstruction (warmer extratropics and slightly cooler tropics relative to the preindustrial era) (22). This agreement may reflect the higher resolution (T159) of the atmospheric model used in that study than for any of those used in the multimodel ensemble (highest resolution of T85) (3). Most of these models do successfully simulate the weak cooling found in our tropical SST stack in response to reduced mean annual insolation at those latitudes (Fig. 1C), but fail to reproduce the evolution of early LIG extratropical SSTs, with model responses to insolation forcing at 130 ka resulting in modest NH warming and no change in the SH extratropics (3, 4), which is opposite to that seen in our reconstructions (Figs. 1 to 3).

The relatively cool-NH versus warm-SH signal during the early LIG was first inferred from speleothem and ice-core records (23) and further documented from SST records (10), including those used in our compilation, and has been attributed to the bipolar seesaw mechanism (23, 24). In particular, a global climate model simulation for 130 ka reproduced this asymmetric temperature signal by perturbing the Atlantic meridional overturning circulation (AMOC) with

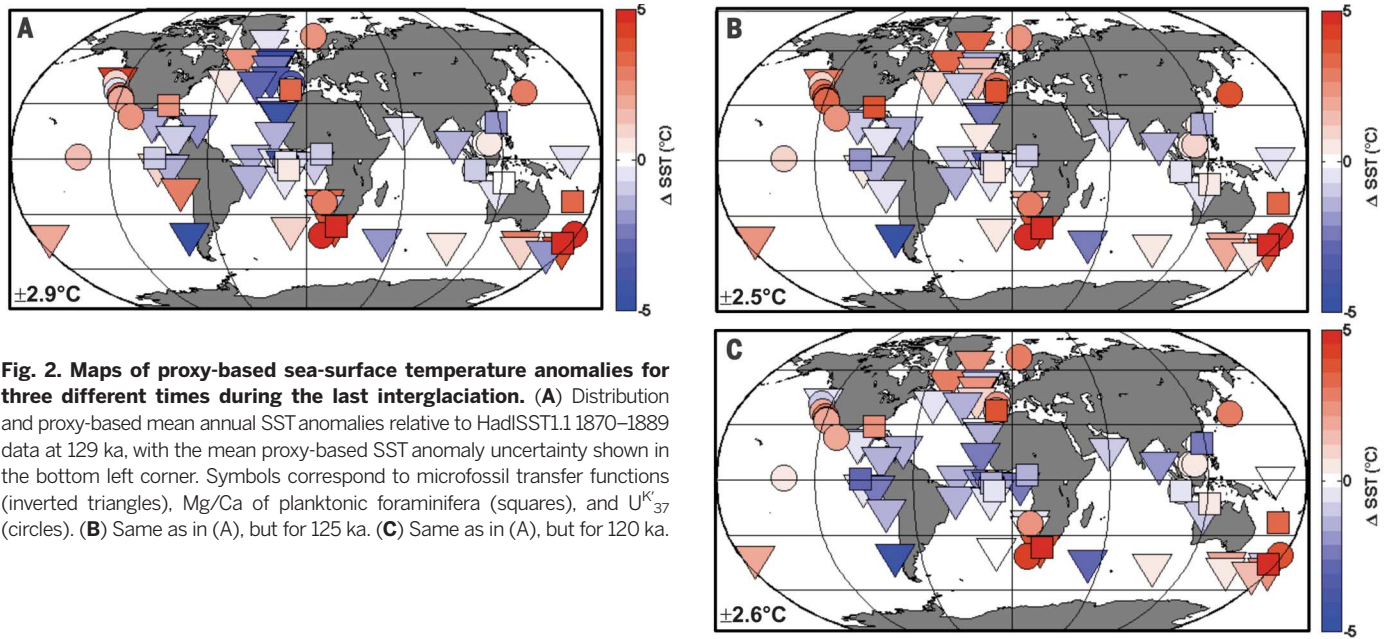


Fig. 2. Maps of proxy-based sea-surface temperature anomalies for three different times during the last interglaciation. (A) Distribution and proxy-based mean annual SST anomalies relative to HadISST1.1 1870–1889 data at 129 ka, with the mean proxy-based SST anomaly uncertainty shown in the bottom left corner. Symbols correspond to microfossil transfer functions (inverted triangles), Mg/Ca of planktonic foraminifera (squares), and U^{K}_{37} (circles). (B) Same as in (A), but for 125 ka. (C) Same as in (A), but for 120 ka.

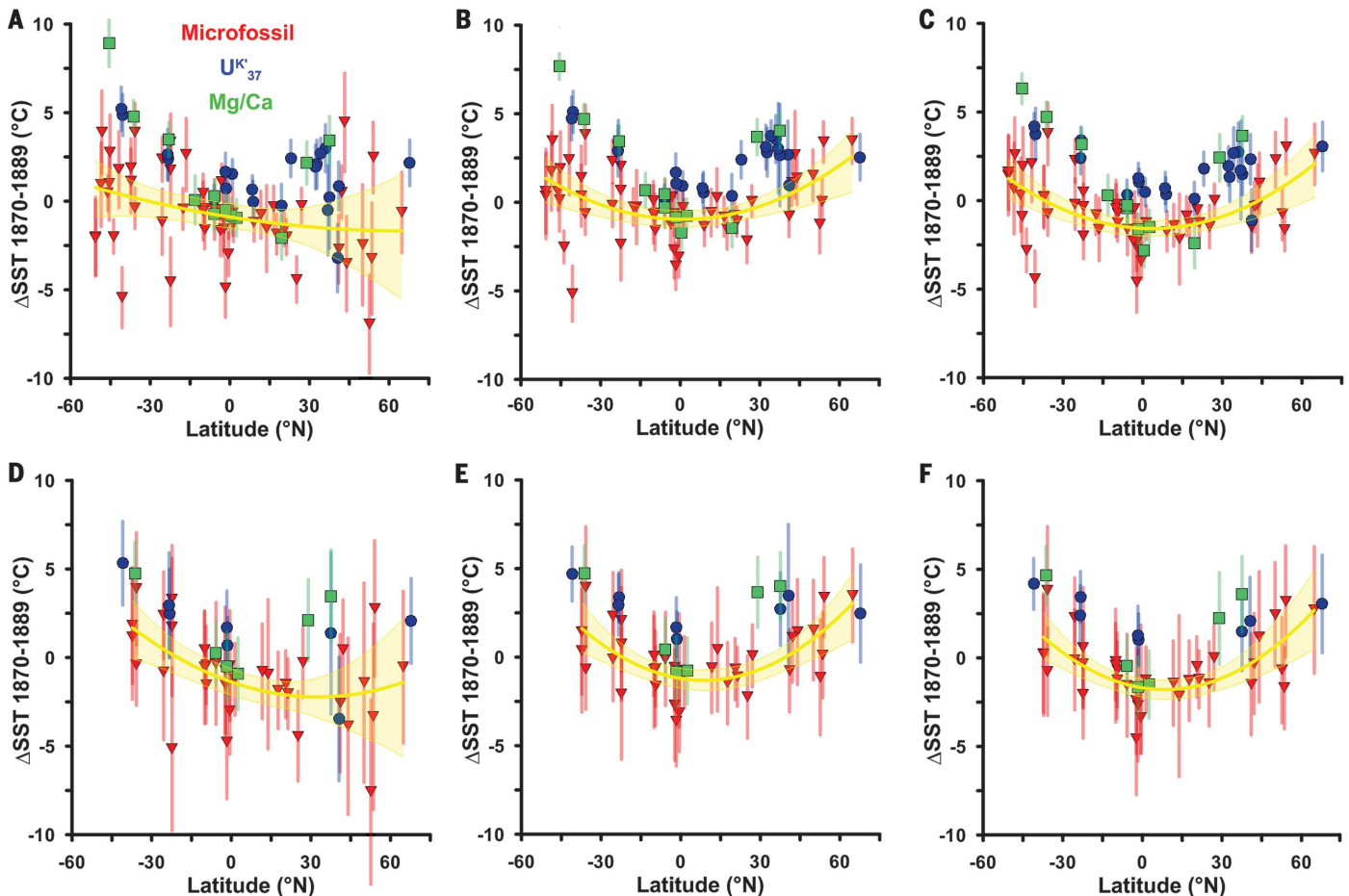


Fig. 3. Proxy-based sea-surface temperature anomalies by latitude for three different times during the last interglaciation. (A) Global proxy-based mean annual SST anomalies with their uncertainties relative to HadISST1.1 1870–1889 data at 129 ka plotted against core-site latitude. Symbols correspond to microfossil transfer functions (red triangles), Mg/Ca of planktonic foraminifera (green squares), and U^{K}_{37} (blue circles). Yellow lines and shading are the fit of a 2nd-order polynomial to the data and its 95% simultaneous functional bounds. (B) Same as in (A), but for 125 ka. (C) Same as in (A), but for 120 ka. (D) Same as in (A), but only those records within the Atlantic basin are plotted. (E) Same as in (D), but for 125 ka. (F) Same as in (D), but for 120 ka.

freshwater forcing from remnant Northern Hemisphere ice sheets (25), which offset NH boreal insolation forcing (4) to sustain cold North Atlantic SSTs while causing warmer SH extratropical SSTs through reduced ocean heat transport. We suggest that the subsequent increase of the AMOC (26) combined with boreal summer insolation forcing (4) to induce NH extratropical warming by 125 ka, particularly in the North Atlantic region. At the same time, the thermal memory of the seesaw response in the SH extratropics, likely associated with sea-ice retreat (27, 28), combined with CO₂ forcing (Fig. 1D) to sustain warm SSTs there, thus resulting in the symmetrical high-latitude warming seen in our reconstruction (Figs. 2B and 3), as well as the warmer global SSTs than those simulated in global climate models that do not include the sea-ice feedback (3, 4). Subsequent high-latitude cooling through the remainder of the LIG (Fig. 1) then likely occurred in response to the dominant obliquity forcing (Fig. 1C) and associated feedbacks (4, 29).

REFERENCES AND NOTES

- Past Interglacials Working Group of PAGES, *Rev. Geophys.* **54**, 162–219 (2016).
- A. Dutton *et al.*, *Science* **349**, aaa4019 (2015).
- D. J. Lunt *et al.*, *Clim. Past* **9**, 699–717 (2013).
- B. L. Otto-Bliesner *et al.*, *Philos. Trans. R. Soc. A* **371**, 20130097–20130097 (2013).
- CLIMAP Project Members *et al.*, *Quat. Res.* **21**, 123–224 (1984).
- P. U. Clark, P. Huybers, *Nature* **462**, 856–857 (2009).
- C. Turney, R. T. Jones, *J. Quat. Sci.* **25**, 839–843 (2010).
- N. P. McKay, J. T. Overpeck, B. L. Otto-Bliesner, *Geophys. Res. Lett.* **38**, L14605 (2011).
- A. Govin *et al.*, *Clim. Past* **8**, 483–507 (2012).
- E. Capron *et al.*, *Quat. Sci. Rev.* **103**, 116–133 (2014).
- S. Barker *et al.*, *Science* **334**, 347–351 (2011).
- Materials and methods are available as supplementary materials.
- L. Skinner, N. Shackleton, *Quat. Sci. Rev.* **24**, 571–580 (2005).
- L. E. Lisiecki, M. E. Raymo, *Paleoceanography* **24**, (2009).
- J. V. Stern, L. E. Lisiecki, *Paleoceanography* **29**, 1127–1142 (2014).
- J. Haslett, A. Parnell, *J. R. Stat. Soc.* **57**, 399–418 (2008).
- N. A. Rayner *et al.*, *J. Geophys. Res.* **108**, 4407 (2003).
- N. J. Abram *et al.*, *Nature* **536**, 411–418 (2016).
- A. Filippova, M. Kienast, M. Frank, R. R. Schneider, *Geochem. Geophys. Geosyst.* **17**, 1370–1382 (2016).
- P. U. Clark *et al.*, *Nat. Clim. Chang.* **6**, 360–369 (2016).
- V. Masson-Delmotte *et al.*, in *Climate Change 2013: The Physical Science Basis: Contribution of Working Group I to the Fifth Assessment Report of the Intergovernmental Panel on Climate Change*, T. F. Stocker *et al.*, Eds. (Cambridge Univ. Press, 2013).
- R. A. Pedersen, P. L. Langen, B. M. Vinther, *Clim. Dyn.* 10.1007/s00382-016-3274-5 (2016).
- M. J. Kelly *et al.*, *Palaeogeogr. Palaeoclimatol. Palaeoecol.* **236**, 20–38 (2006).
- V. Masson-Delmotte *et al.*, *Quat. Sci. Rev.* **29**, 113–128 (2010).
- E. J. Stone *et al.*, *Clim. Past* **12**, 1919–1932 (2016).
- E. Böhm *et al.*, *Nature* **517**, 73–76 (2015).
- E. W. Wolff *et al.*, *Quat. Sci. Rev.* **29**, 285–295 (2010).
- M. D. Holloway *et al.*, *Nat. Commun.* **7**, 12293 (2016).
- A. Timmermann *et al.*, *J. Clim.* **27**, 1863–1875 (2014).
- R. Schneider, J. Schmitt, P. Köhler, F. Joos, H. Fischer, *Clim. Past* **9**, 2507–2523 (2013).
- S. Eggleston, J. Schmitt, B. Bereiter, R. Schneider, H. Fischer, *Paleoceanography* **31**, 434–452 (2016).

ACKNOWLEDGMENTS

Research was supported by an NSF Graduate Research Fellowship to J.S.H. under NSF grant 1314109-DGE and by NSF grants 1335197 and 1503032 to P.U.C. F.H. was supported by NSF grant AGS-1502990 and by the National Oceanic and Atmospheric Administration's Climate and Global Change Postdoctoral Fellowship program, administered by the University Corporation for Atmospheric Research. We acknowledge high-performance computing support from Yellowstone (ark:/85065/d7wd3xhc) provided by the National Center for Atmospheric Research's Computational and Information Systems Laboratory, sponsored by the NSF. This research used resources of the Oak Ridge Leadership Computing Facility at the Oak Ridge National Laboratory, which is supported by the Office of Science of the U.S. Department of Energy under contract no. DE-AC05-00OR22725. We thank the members of the Past Global Changes–Paleoclimate Modelling Intercomparison Project (PAGES-PMIP) Working Group on Quaternary Interglacials, P. Bakker, H. A. Bauch, A. E. Carlson, M. S. Hoecker-Martinez, S. A. Marcott, H. L. O. McClelland, N. McKay, A. C. Mix, N. G. Pisias, and J. D. Shakun for helpful discussions. The authors report no conflicts of interest. J.S.H. and P.U.C. designed the study and wrote the manuscript with help from A.C.P. and F.H. We acknowledge insightful comments from two anonymous reviewers. The data reported in this paper are tabulated in the supplementary materials.

SUPPLEMENTARY MATERIALS

www.sciencemag.org/content/355/6322/276/suppl/DC1
Materials and Methods
Figs. S1 to S43
Tables S1 and S2
References (32–118)
Data File S1

19 August 2016; accepted 21 December 2016
10.1126/science.aai8464

Regional and global sea-surface temperatures during the last interglaciation

Jeremy S. Hoffman, Peter U. Clark, Andrew C. Parnell and Feng He

Science **355** (6322), 276-279.
DOI: 10.1126/science.aai8464

Sea surface temperatures of the past

Understanding how warm intervals affected sea level in the past is vital for projecting how human activities will affect it in the future. Hoffman *et al.* compiled estimates of sea surface temperatures during the last interglacial period, which lasted from about 129,000 to 116,000 years ago. The global mean annual values were $\sim 0.5^{\circ}\text{C}$ warmer than they were 150 years ago and indistinguishable from the 1995–2014 mean. This is a sobering point, because sea levels during the last interglacial period were 6 to 9 m higher than they are now.

Science, this issue p. 276

ARTICLE TOOLS

<http://science.sciencemag.org/content/355/6322/276>

SUPPLEMENTARY MATERIALS

<http://science.sciencemag.org/content/suppl/2017/01/23/355.6322.276.DC1>

RELATED CONTENT

<file:/contentpending:yes>

REFERENCES

This article cites 100 articles, 16 of which you can access for free
<http://science.sciencemag.org/content/355/6322/276#BIBL>

PERMISSIONS

<http://www.sciencemag.org/help/reprints-and-permissions>

Use of this article is subject to the [Terms of Service](#)

Science (print ISSN 0036-8075; online ISSN 1095-9203) is published by the American Association for the Advancement of Science, 1200 New York Avenue NW, Washington, DC 20005. The title *Science* is a registered trademark of AAAS.

Copyright © 2017, American Association for the Advancement of Science